PHOTONIC SENSORS / Vol. 6, No. 2, 2016: 137−142

A High Sensitivity Pressure Sensor Based on Two-Dimensional Photonic Crystal

Shangbin TAO, Deyuan CHEN*, Juebin WANG, Jing QIAO, and Yali DUAN

Nangjing University of Posts and Telecommunications, Nanjing, 210009, China

*Corresponding author: Deyuan CHEN E-mail: chendy@njupt.edu.cn

Abstract: In this paper, we propose and simulate a pressure sensor based on two-dimensional photonic crystal with the high quality factor and sensitivity. The sensor is formed by the coupling of two photonic crystal based waveguides and one nanocavity. The photonic crystal with the triangular lattice is composed of GaAs rods. The detailed structures of the waveguides and nanocavity are optimized to achieve better quality factor and sensitivity of the sensor. For the optimized structures, the resonant wavelength of the sensor has a linear redshift as increasing the applied pressure in the range of 0 – 2 GPa, and the quality factor keeps unchanged nearly. The optimized quality factor is around 1500, and the sensitivity is up to 13.9 nm/GPa.

Keywords: Photonic crystal; waveguide; nanocavity; pressure sensor

Citation: Shangbin TAO, Deyuan CHEN, Juebin WANG, Jing QIAO, and Yali DUAN, "A High Sensitivity Pressure Sensor Based on Two-Dimensional Photonic Crystal," *Photonic Sensors*, 2016, 6(2): 137–142.

1. Introduction

Eli Yablonovitch and Sajeev John proprosed the conception of photonic crystal (PhC) in 1980s [1], which can mold the flow of light. Photonic crystal is a structure in which a periodic variation in refractive index occurs at the scale of the wavelength of light in one, two or three directions. PhCs have many attractive characteristics such as photonic bandgap (PBG), localization effect, and refraction effect. By introducing point defect and/or line defect, PhC-based devices can be made [2], such as PhC-based waveguide [3−5], nanocavity [6−8], low threshold lasers [9−12], PhC-based filter [13−15], PhC fibers [16−19], optical sensors, and so on.

In last few years, a large number of research and investigations have shown that PhC can also be used to make optical sensors. Yang *et al.* presented an electro-optical sensor based on a slotted 2D-PhC waveguide which exhibited over 30-times sensitivity enhancement and about 6.6 times improvement in quality factor compared with the W1-PhC waveguide based electro optical sensor [20]. Xu *et al.* designed a micro displacement sensor based on the 2D-PhC line-defect resonant cavity structure which could be integrated in a micro-electro-mechanical system [21]. Besides, PhC can be used to design a pressure sensor. Shanthi *et al.* demonstrated a 2D-PhC based pressure sensor whose sensitivity could reach 2 nm/GPa and dynamic range could reach 7 GPa [22]. Olyaee *et al.* designed a 2D-PhC pressure sensor which had the sensitivity of 8 nm/GPa and wide linearity range between 0 and 10 GPa.

In this paper, we design and simulate a 2D-PhC based pressure sensor using the coupling of two

Received: 18 January 2016 / Revised: 8 March 2016

DOI: 10.1007/s13320-016-0316-x
Article type: Regular

PhC-based waveguides with a PhC-based nanocavity. The sensor is made of GaAs with the stronger photo-elastic effect. The refractive index of GaAs varies under pressure, and the resonant wavelength of the microcavtiy made of GaAs rods shifts. The sensor properties such as the quality factor, resonant wavelength, transmittance, sensitivity, and dynamic range are investigated. The electromagnetic analysis of the sensor has been conducted by applying a commercial finite element method code, i.e. COMSOL multiphysics.

2. Pressure effect analysis

The sensor principle is based on the change in the refractive index of the material induced by the photoelastic effect, piezoelectric effect, and eletrooptic effect. The change in the refractive index will modify the resonant wavelength of the structure. And it is found that the variation of the refractive index is mainly due to the photo-elastic effect [23].

The relationship between the refractive index and the stress can be expressed as follows [22−24]:

$$\begin{pmatrix} n_{xx} \\ n_{yy} \\ n_{zz} \\ n_{yz} \\ n_{xz} \\ n_{xy} \end{pmatrix} = \begin{pmatrix} n_0 \\ n_0 \\ n_0 \\ 0 \\ 0 \\ 0 \end{pmatrix} - \begin{pmatrix} C_1 & C_2 & C_2 & 0 & 0 & 0 \\ C_2 & C_1 & C_2 & 0 & 0 & 0 \\ C_2 & C_2 & C_1 & 0 & 0 & 0 \\ 0 & 0 & 0 & C_3 & 0 & 0 \\ 0 & 0 & 0 & 0 & C_3 & 0 \\ 0 & 0 & 0 & 0 & 0 & C_3 \end{pmatrix} \begin{pmatrix} \sigma_{xx} \\ \sigma_{yy} \\ \sigma_{zz} \\ \sigma_{yz} \\ \sigma_{xz} \\ \sigma_{xy} \end{pmatrix} \quad (1)$$

where C_1, C_2, and C_3 are defined as

$$C_1 = n_0^3 (p_{11} - 2\upsilon p_{12})/2E \quad (2)$$

$$C_2 = n_0^3 [p_{12} - \upsilon(p_{11} + p_{12})]/2E \quad (3)$$

$$C_3 = n_0^3 p_{44}/2G \quad (4)$$

where p_{11}, p_{12}, and p_{44} are strain-optic constants, E, G, and υ represent the Youngs modulus, shear modulus, and Poissons ratio. σ_{ij} stands for the pressure along ij direction, and n_{ij} denotes the refractive index along ij direction.

We assume that the pressure is orthogonal to the photonic crystal plane and applied only in one direction, which means that the pressure is distributed uniformly and the whole structure is under the hydrostatic pressure state, therefore:

$$\sigma_{xx} = \sigma_{yy} = \sigma_{zz} = \sigma \quad (5)$$

$$\sigma_{xy} = \sigma_{xz} = \sigma_{yz} = 0 \quad (6)$$

So (1) can be simplified to

$$n = n_o - (C_1 + 2C_2)\sigma \quad (7)$$

where n_0 is the refractive index without the applied pressure.

For GaAs, we have [23]

$$n = 3.43 \quad (8)$$

$$p_{11} = -0.165 \quad (9)$$

$$p_{12} = -0.140\,. \quad (10)$$

3. Design and analysis of 2D-PhC pressure sensor structure

3.1 Design of 2D-PhC

The structure of the 2D-PhC is shown in Fig. 1(a). It is of 15×20 triangular lattice arrays of GaAs rods in air. The photonic crystal lattice constant and rods radius are 540 nm and 130 nm, respectively.

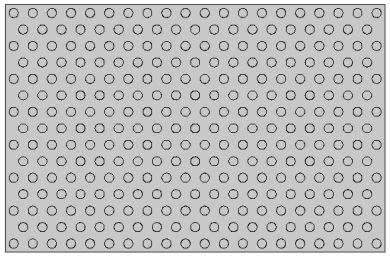

(a)

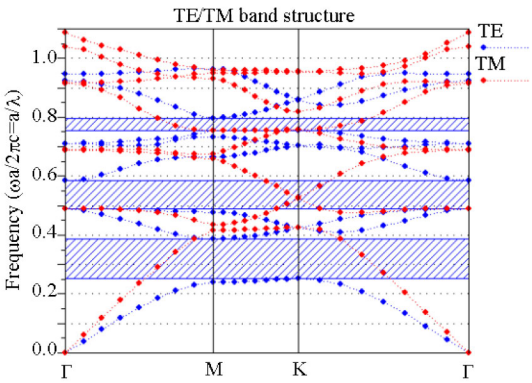

(b)

Fig. 1 Two-dimensional photonic crystal: (a) schematic diagram and (b) TE/TM mode band structure of the 2D-PhC.

The electromagnetic analysis of the 2D-PhC

structure has shown a large bandgap for TE polarization between 0.251(a/λ) and 0.386(a/λ) as shown in Fig. 1(b).

Two line defects are introduced by removing GaAs rods in order to form the input and output waveguides as shown in Fig. 2. These two waveguides are coupled through a nanocavity which is formed by removing one GaAs rod between the two waveguides. The port marked "input" with an arrow in Fig. 2 is the input port. The light source is put at the input port in order to excite the structure. The port marked "output" in Fig. 2 is the output port. The photonic detector is placed at the output port to detect the output light so that the resonant wavelength of the structure can be analyzed. The part of the sensor, i.e., the waveguides ends and the nanocavity marked in Fig. 2 by the dotted lines are studied and optimized in order to achieve better performance.

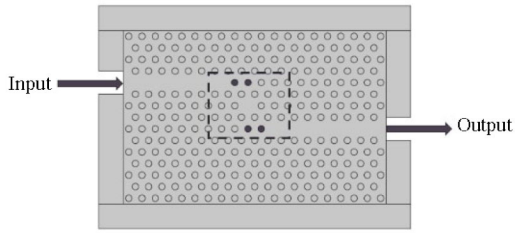

Fig. 2 Schematic diagram of the 2D-PhC sensor.

3.2 Design of waveguides and nanocavity

The detailed structure which is marked by dotted lines in Fig. 2 can influence the performance of the sensor. So the waveguides are optimized at their ends as shown in Fig. 3, the enlarged view of the coupling part. Three cases are considered. In Case (a), the rods numbered 1 and 1', and 2 and 2' are kept. In Case (b), rods numbered 1 and 1' are removed, and 2 and 2' are kept. In Case (c), rods numbered 1 and1', and 2 and 2' are all removed.

The transmission spectra of the sensors with different waveguides ends are displayed in Fig. 4. It is obvious that Case (c) cannot be used for its worst transmittance, multi-modes, and lowest quality factor. So no more GaAs rods should be removed. For Case (a), the quality factor is better up to 480, while the transmittance is low; for Case (b), the quality factor is low to 130, while transmittance is better.

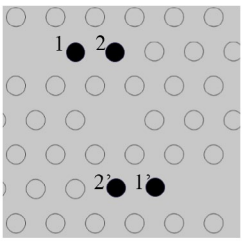

Fig. 3 Enlarged views of the sensor which is marked by dotted lines in Fig. 2.

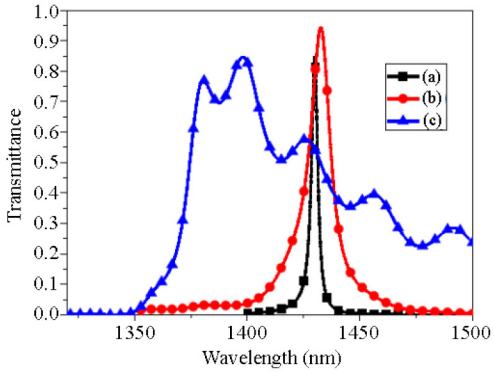

Fig. 4 Transmission spectrum of the 2D-PhC sensor with different coupling parts of Cases (a), (b), and (c).

We also analyze the case that less GaAs rods are removed to form the waveguide. The corresponding transmittance is even lower because most of the light is reflected.

Besides, the structure of the nanocavity determines the quality factor when the lattice constant and radius of rods are decided. By properly designing the nanocavity, the high quality factor and sensitivity may be achieved.

Removing one GaAs rod as is shown in Fig. 2 can be the simplest nanocavity. But the quality factor is too low, so it is necessary to optimize the structure of the nanocavity. In order to increase the quality factor and the sensitivity, the structure of the nanocavity is changed. And two small GaAs rods with the radius of 65 nm are placed inside the nanocavity as is shown in Fig. 5.

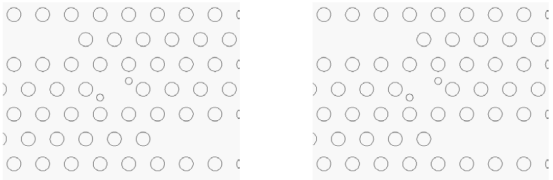

(a) (b)

Fig. 5 Enlarged coupling part of Cases (a) and (b).

3.3 Performance of the sensor

For both the structures of Cases (a) and (b) shown in Fig. 5, the pressure is applied with a step of 0.5 GPa from 0 to 2 GPa to study the performance of the sensors.

Figure 6 shows the transmittance of the sensor for Case (a) under different pressures from 0 to 2 GPa. It is clear that with increasing the pressure, the coupling resonant mode red-shifts, the transmittance decreases from 96% to 72%, and the quality factor decreases from 1140 to 838. The resonant mode wavelength with pressure has been dotted in Fig. 7. An obvious linear relationship can be observed, allowing linear measurements of the pressure. Therefore, it is relatively proper to estimate the sensor sensitivity S as the ratio of the resonant wavelength variation to the applied pressure variation, i.e., the slop of the curve:

$$S = \frac{\Delta\lambda}{\Delta P}. \tag{11}$$

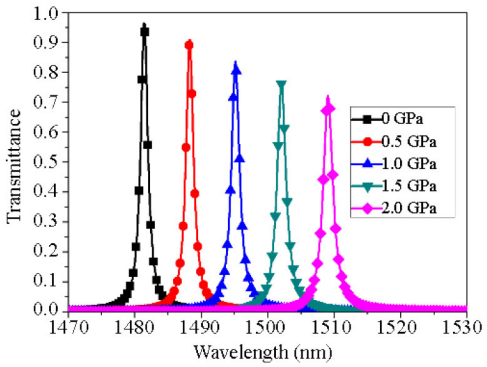

Fig. 6 Transmission spectrum for different applied pressures.

In the case, S equals 13.7 nm/GPa. It seems to have the better performance parameter, but the transmittance drops when increasing pressure. When applying 2 GPa pressure, the transmittance drops to 72%, which is unacceptable.

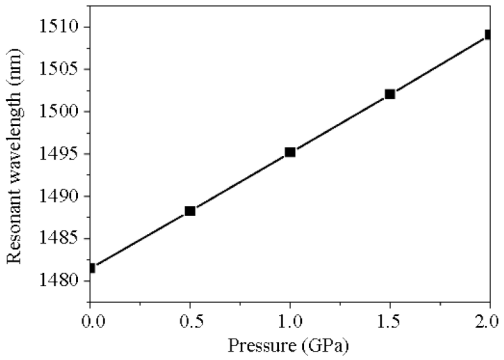

Fig. 7 Linear relationship between the resonant wavelength and pressure in the range of 0 to 2 Gpa.

For Case (b), the transmittance spectra of the sensor under different pressures are shown in Fig. 8. With increasing pressure, the resonant wavelength has a linear redshift, and the transmittance and the quality factor change slightly.

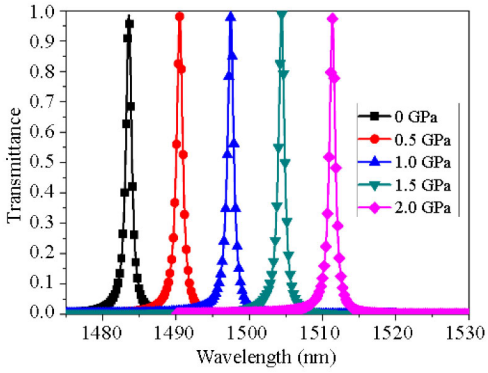

Fig. 8 Transmission spectrum for different applied pressures.

Also, the relationship between the resonant mode wavelength and pressure in the range of 0 to 2 GPa has been plotted in Fig. 9. It is clear that the resonant wavelength shifts linearly with the applied pressure, allowing linear measurements of the pressure. So we can calculate the quality factor to be around 1500, and the sensitivity is up to 13.9 nm/GPa.

According to the quality factor and the sensitivity of the above two cases, Case (b) is the better one for the pressure sensor. The parameters are summarized in Table 1.

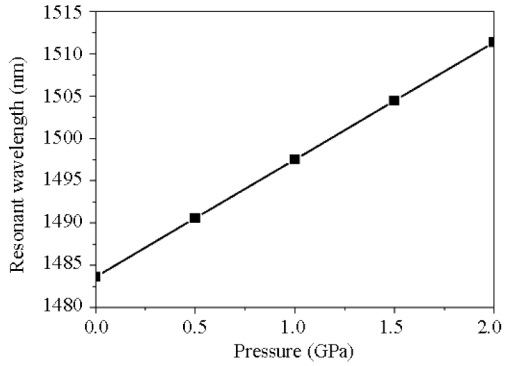

Fig. 9 Linear relationship between resonant wavelength and pressure in the range of 0 to 2 Gpa.

Table 1 Parameters of the sensor.

Parameters	Values
Lattice constant a	540 nm
Radius of the rod r	130 nm
Radius of the rod in the cavity	65 nm
Size	20×15
Refractive index of GaAs rod n_o	3.43
Refractive index of background	1
Polarization	TE
PBG	0.251–0.386(a/λ)

The comparison between the proposed pressure sensor and similar sensors is presented in Table 2.

Table 2 Comparison between the proposed sensor and other similar sensors.

Parameters	Quality factor	Sensitivity (nm/GPa)
Ref.[22]	75.5	2
Ref.[24]	1470	8
Proposed sensor	1500	13.9

4. Conclusions

We have proposed the design of a pressure sensor based on the two-dimensional photonic crystal with the triangular lattice of GaAs rods surrounded by air. This sensor is constructed with PhC-based waveguides coupling with a nanocavity. The quality factor increases to 1500 by modifying the lattice constant, radius of GaAs rods, and the structure of waveguides and nanocavity. The refractive index of GaAs changes along with the applied pressure due to the photo-elastic effect. Through simulation, we have found that the resonant wavelength shifts and follows a linear law. The quality factor is around 1500, and the sensitivity is about 13.9 nm/GPa under the dynamic range between 0 and 2 GPa. This sensor can be used in detecting occations such as long-distance pipeline strain monitoring or other sensing applications because of its high sensitivity and fast responding.

Acknowledgment

This work was supported by the NSFC (National Natural Science Foundation of China) (Nos. 61302101 and 61306003), the NSF (Natural Science Fundation) of Jiangsu Province of China (No. BK20130874), the NSF of the Jiangsu Higher Education Institutions (No. 13KJB510025), GSRIP (Graduate Student Research and Innovation Project) of Jiangsu Province (Nos. KYLX_0801 and SJLX15_0376), NUPTSP (Nanjing University of Posts and Telecommunications Science Project) (No. NY214051).

References

[1] E. Yablonovitch, "Inhibited spontaneous emission in solid-state physics and electronics," *Physics Review Letters*, 1987, 58(20): 2059–2062.

[2] J. D. Joannopoulos, R. D. Meade, and J. N. Winn, *Photonic crystal: modling of flow of light*. Princeton, NJ: Princeton University Press, 1995.

[3] A. Mekis, J. C. Chen, I. Kurland, S. Fan, P. R. Villeneuve, and J. D. Joannopoulos, "High transmission through sharp bends in photonic crystal waveguides," *Physical Review Letters*, 1996, 77(18): 3787–3790.

[4] M. Tokushima, H. Kosaka, A. Tomita, and H. Yamada, "Lightwave propagation through a 120° sharply bent single-line-defect photonic crystal waveguide," *Applied Physics Letters*, 2000, 76(8): 952–954.

[5] A. Lavrinenko, P. Borel, L. Frandsen, M. Thorhauge,

A. Harpth, M. Kristensen, *et al*., "Comprehensive FDTD modelling of photonic crystal waveguide components," *Optics Express*, 2004, 12(2): 234–248.

[6] N. Susumu, C. Alongkarn, and I. Masahiro, "Trapping and emission of photons by a single defect in a photonic bandgap structure," *Nature*, 2000, 407(6804): 608–610.

[7] Y. Akahane, T. Asano, B. Song, and N. Susumu, "High-Q photonic nanocavity in a two-dimensional photonic crysal," *Nature*, 2003, 425(6961): 944–947.

[8] K. Srinivasan, P. Barclay, O. Painter, J. Chen, A. Y. Cho, and C. Gmach, "Experimental demonstration of a high quality factor photonic crystal microcavity," *Applied Physics Letters*, 2003, 83(10): 1915–1917.

[9] M. Loncar, T. Yoshie, A. Scherer, P. Gogna, and Y. Qiu, "Low-threshold photonic crystal laser," *Applied Physics Letters*, 2002, 81(15): 2680–2682.

[10] H. G. Park, S. H. Kim, S. H. Kwon, Y. Ju, J. Yang, J. Baek, *et al*., "Electrically driven single-cell photonic crystal laser," *Science*, 2004, 305(5689): 1444–1447.

[11] O. Painter, A. Husain, A. Scherer, P. T. Lee, I. Kim, J. D. O'Brien, *et al*., "Lithographic tuning of a two-dimensional photonic crystal laser array," *IEEE Photonics Technology Letters*, 2000, 12(9): 1126–1128.

[12] K. Inoue, M. Sasada, J. Kawamata, K. Sakoda, and J. W. Haus, "A two-dimensional photonic crystal laser," *Applied Physics Letters*, 1999, 38(2B): 157–159.

[13] N. Mec, P. Kuzel, L. Duvillaret, A. Pashkin, M. Dressel, and M. T. Sebastian, "Highly tunable photonic crystal filter for the terahertz range," *Optics Letters*, 2005, 30(5): 549–551.

[14] W. Li, Y. Fu, Q. Zhang, and D. F. Shi, "Filtering performance comparision of two types of photonic crystal filter," *Laser & Infrared*, 2010, 40(7): 762–765.

[15] Y. Kanamori, N. Matsuyama, and K. Hane, "Resonant wavelength tuning of a pitch-variable 1-D photonic crystal filter at telecom frequencies," *IEEE Photonics Technology Letters*, 2008, 20(13): 1136–1138.

[16] J. C. Knight, T. A. Birks, P. S. Russell, and D. M. Atkin, "All-silica single-mode optical fiber with photonic crystal cladding," *Optics Letters*, 1996, 21(19): 1547–1549.

[17] R. F. Cregan, B. J. Mangan, and J. C. Knight, "Single-mode photonic band gap guidance of light in air," *Science*, 1999, 285(5433): 1537–1539.

[18] S. Kunimasa, S. Yuichiro, and K. Masanori, "Coupling characteristics of dual-core photonic crystal fiber couplers," *Optics Express*, 2003, 11(24): 3188–3195.

[19] P. Russell, "Photonic crystal fibers," *Journal of Lightwave Technology*, 2007, 24(12): 4729–4749.

[20] D. Yang, H. Tian, and Y. Ji, "The study of electro-optical sensor based on slotted photonic crystal waveguide," *Optics Communications*, 2011, 284(20): 4986–4990.

[21] Z. Xu, L. Cao, C. Gu, Q. He, and G. Jin, "Micro displacement sensor based on line-defect resonant cavity in photonic crystal," *Optics Express*, 2006, 14(1): 298–305.

[22] K. V. Shanthi and S. Robinson, "Two-dimensional photonic crystal based sensor for pressure sensing," *Photonic Sensors*, 2014, 3(3): 248–253.

[23] M. Huang, "Stress effects on the performance of optical waveguides," *Solids & Structures*, 2003, 40(7): 1615–1632.

[24] S. Olyaee and A. A. Dehghani, "High resolution and wide dynamic range pressure sensor based on two-dimensional photonic crystal," *Photonic Sensors*, 2012, 2(1): 92–96.

[25] optical waveguides," *Solids & Structures*, 2003, 40(7): 1615–1632.

[26] S. Olyaee and A. A. Dehghani, "High resolution and wide dynamic range pressure sensor based on two-dimensional photonic crystal," *Photonic Sensors*, 2012, 2(1): 92–96.